Regulation of fatty acid trafficking in liver by thioesterase superfamily member 1[S]

Anal Desai,* Michele Alves-Bezerra,* Yingxia Li,* Cafer Ozdemir,† Curtis J. Bare,* Yue Li,§ Susan J. Hagen,§ and David E. Cohen[1,*]

Joan & Sanford I. Weill Department of Medicine,* Weill Cornell Medical College, New York, NY 10021; Department of Biochemistry,† Boston University School of Medicine, Boston, MA 02118; and Department of Surgery,§ Beth Israel Deaconess Medical Center, Harvard Medical School, Boston, MA 02215

Abstract **Thioesterase superfamily member 1 (Them1) is an acyl-CoA thioesterase that is highly expressed in brown adipose tissue, where it functions to suppress energy expenditure. Lower Them1 expression levels in the liver are upregulated in response to high-fat feeding. *Them1*$^{-/-}$ mice are resistant to diet-induced obesity, hepatic steatosis, and glucose intolerance, but the contribution of Them1 in liver is unclear. To examine its liver-specific functions, we created conditional transgenic mice, which, when bred to *Them1*$^{-/-}$ mice and activated, expressed Them1 exclusively in the liver. Mice with liver-specific Them1 expression exhibited no changes in energy expenditure. Rates of fatty acid oxidation were increased, whereas hepatic VLDL triglyceride secretion rates were decreased by hepatic Them1 expression. When fed a high-fat diet, Them1 expression in liver promoted excess steatosis in the setting of reduced rates of fatty acid oxidation and preserved glycerolipid synthesis. Liver-specific Them1 expression did not influence glucose tolerance or insulin sensitivity, but did promote hepatic gluconeogenesis in high-fat-fed animals. This was attributable to the generation of excess fatty acids, which activated PPARα and promoted expression of gluconeogenic genes.[JLR] These findings reveal a regulatory role for Them1 in hepatocellular fatty acid trafficking.**—Desai, A., M. Alves-Bezerra, Y. Li, C. Ozdemir, C. J. Bare, Y. Li, S. J. Hagen, and D. E. Cohen. **Regulation of fatty acid trafficking in liver by thioesterase superfamily member 1. *J. Lipid Res.* 2018.** 59: **368–379.**

Supplementary key words lipids • nonalcoholic fatty liver disease • obesity • triglycerides • fatty acid/metabolism • fatty acid/oxidation • very low density lipoprotein • fatty acyl-CoA

Upon uptake or synthesis within hepatocytes, long-chain FFAs are activated by long-chain acyl-CoA synthetases (ACSLs) to form fatty acyl-CoA molecules, which may then become incorporated into complex lipids or undergo oxidation within mitochondria or peroxisomes. This thioesterification reaction is reversed by acyl-CoA thioesterases (ACOTs) (1, 2), a family of enzymes with well-characterized biochemical activities, but with biological functions that remain largely unexplored (2). Multiple ACSL and ACOT isoforms are expressed in cells, suggesting a role of these enzymes in the formation of distinct pools of fatty acids/acyl-CoAs to be channeled into specific metabolic pathways (1).

Thioesterase superfamily member 1 (Them1) [synonyms: brown fat inducible thioesterase (BFIT), steroidogenic acute regulatory protein-related lipid transfer (START) domain 14 (StarD14)/Acot11] is enriched in mouse brown adipose tissue (BAT), and its expression is markedly upregulated by cold ambient temperatures (3, 4). Genetic disruption of Them1 in mice resulted in increased energy expenditure, as well as resistance to diet-induced obesity and diabetes (4). Suppression of energy expenditure in BAT occurred when Them1 limited the flux of fatty acids from lipid droplets (LDs) to mitochondria for β-oxidation by inhibiting lipolysis of LD triglycerides (TGs) (5).

The phenotypes of *Them1*$^{-/-}$ mice were also notable for resistance to diet-induced insulin resistance and to hepatic steatosis (4). In the absence of Them1 expression, livers of *Them1*$^{-/-}$ mice exhibited attenuated endoplasmic reticulum stress and altered transcription of genes involved in fatty acid metabolism, suggestive of decreased lipogenesis. Although expressed at much lower levels than in BAT, the

This work was supported by National Institute of Diabetes and Digestive and Kidney Diseases Grant R01 DK103046 (S.J.H. and D.E.C.) and Harvard Digestive Diseases Center Grant P30 DK034854. M.A-B. was the recipient of an American Liver Foundation Non-Alcoholic Steatohepatitis Fatty Liver Disease Postdoctoral Research Fellowship Award; C.O. was the recipient of an American Liver Foundation Thomas F. Nealon, III Postdoctoral Research Fellowship Honoring Zachery Rue; and Y. L. was the recipient of an American Liver Foundation Irwin M. Arias, MD Postdoctoral Research Fellowship. The contents are solely the responsibility of the authors and do not necessarily represent the official views of the National Institutes of Health.

Manuscript received 25 October 2017 and in revised form 4 December 2017.

Published, JLR Papers in Press, December 5, 2017
DOI https://doi.org/10.1194/jlr.M081455

Abbreviations: ACOT, acyl-CoA thioesterase; ACSL, acyl-CoA synthetase long-chain; APOB, apolipoprotein-B; AUC, area under the curve; BAT, brown adipose tissue; CPT1, carnitine palmitoyltransferase-1; EGFP, enhanced green fluorescent protein; FABP1, fatty acid binding protein 1; FATP, fatty acid transport protein; GPAT, glycerol-3-phosphate acyltransferase; GTT, glucose tolerance test; ITT, insulin tolerance test; KO + LTg mice, *Them1*$^{-/-}$*;L-Them1Tg* mice; LD, lipid droplet; OCR, oxygen consumption rate; PL, phospholipid; PTT, pyruvate tolerance test; qPCR, quantitative PCR; Them1, thioesterase superfamily member 1; TG, triglyceride.

[1]To whom correspondence should be addressed.
e-mail: dcohen@med.cornell.edu

[S] The online version of this article (available at http://www.jlr.org) contains a supplement.

hepatic expression of Them1 is nevertheless appreciable (4, 6). Experiments using primary cultured hepatocytes left open the possibility of cell-autonomous effects of Them1 (4), but whether these were due to Them1 expression in the liver per se or were secondary to increases in energy expenditure remains unclear. A direct role for Them1 in liver is supported by the observation that Them1 mRNA is upregulated 13-fold in response to high-fat feeding (7). To explore its direct role in hepatic lipid metabolism, we created a conditional Them1 transgenic C57BL/6J mouse, which, when bred to a whole-body C57BL/6J *Them1*$^{-/-}$ mouse, enabled tissue-specific expression. We crossed these mice with C57BL/6J albumin-cre transgenic mice to selectively overexpress Them1 in the liver. Our results demonstrate that, in chow-fed mice, hepatic Them1 promoted fatty acid oxidation, while limiting TG storage and secretion. By contrast, in response to high-fat feeding, Them1 function promotes TG storage at the expense of oxidation, thereby promoting hepatic steatosis. The hepatic expression of Them1 did not influence whole-body energy expenditure, glucose tolerance, or insulin resistance. However, liver-Them1 expression did promote hepatic glucose production in response to high-fat feeding, apparently by activating PPARα to promote the expression of gluconeogenic genes.

MATERIALS AND METHODS

Animals and diets

Transgenic mice were prepared by standard techniques. The 1,785 bp coding region sequence of *Mus musculus Acot11* cDNA (NM_025590.4) was cloned into the SalI sites of the pCAG-Z-EGFP vector (Origene, Rockville, MD), which consisted of a LacZ and 3′ polyA stop sequence flanked by loxP, mouse Them1, internal ribosome entry site (IRES), and enhanced green fluorescent protein (EGFP), driven sequentially by a chicken-β-actin promoter. The orientation was confirmed by restriction digest using EcoRI (New England Biolabs, Ipswich, MA). This construct allowed for the expression of Them1 in a tissue-specific manner using cre recombinase to excise T-LacZ and enable the transcription of mouse Them1 and EGFP. The IRES element provided for the independent translation of Them1 and EGFP. Assembly of the construct was verified by PCR and nucleotide sequencing. The plasmid was then linearized by using SpeI and Afl2 and injected into pronuclei of eggs from C57BL/6J female mice (Partners Transgenic Core Facility, Harvard Medical Area Core Management System, Boston, MA). Offspring were screened for X-gal staining of tail tissue. Litters were genotyped for integration of the transgene by PCR analysis from tail genomic DNA using the following primers: forward, 5-GTGCTGGTTATTGTGCTG-3, and reverse, 5-GACGACAGTATCGGCCTC-3. Mice that were positive for the transgene were then screened by quantitative PCR (qPCR) to determine copy number. Mice with two copies of the transgene were selected for breeding. Conditional Them1 transgenic (*c-Them1Tg*) mice were crossed with *Them1*$^{-/-}$ mice (4) that were backcrossed >20 generations to the C57BL/6J background in order to create *Them1*$^{-/-}$*;c-Them1Tg* (KO) mice. KO mice were then crossed with B6.Cg-Tg(Alb-cre)21Mgn/J mice (The Jackson Laboratory, Bar Harbor, ME) to generate liver-specific *Them1*$^{-/-}$*;L-Them1Tg* (KO + LTg) mice. The presence of cre was determined by PCR analysis using the primers specified by The Jackson Laboratory.

Mice were housed in a barrier facility on a 12 h light/dark cycle. At 4–5 weeks of age, male mice were weaned and fed normal chow or a high-fat diet (60% kcal from fat; Research Diets Inc., New Brunswick, NJ). Mice were sacrificed following a 4 h fast, and plasma and tissues were then harvested for immediate use or for storage at −80°C. Hepatocytes were isolated from 12-week-old mice and cultured as previously described (8). Animal use and euthanasia protocols were approved by both Harvard Medical School and Weill Cornell Medical College.

Histopathology

Liver samples were fixed in 4% paraformaldehyde and sectioned. H&E staining was performed by using standard techniques by the Histology Core at the Beth Israel Deaconess Medical Center (Harvard Medical School, Boston, MA). Images were taken by using an Axioimager 2 widefield microscope (Carl Zeiss, Inc., Thornwood, NY).

Biochemical analyses

Enzymatic assay kits were used to measure plasma and hepatic concentrations of TG, FFA, total cholesterol, free cholesterol, phospholipid (PL)-C (Wako Diagnostics, Mountain View, CA), and β-hydroxybutyrate (Stanbio Laboratories, Boerne, TX) (9). Plasma concentrations of insulin were measured by using an ELISA kit (Crystal Chem, Downers Grove, IL), according to the manufacturer's protocol. Protein concentrations were determined by using a BCA reagent (Thermo Fisher Scientific, Springfield Township, NJ).

ACOT activity

ACOT activities were measured in liver homogenates as previously described (10). Briefly, frozen liver samples (30 mg) were homogenized in buffer containing: 20 mM Tris (pH 8.0), 137 mM NaCl, 1 mM EDTA, and 10% (vol/vol) glycerol. Homogenates were sonicated for 20 s and then centrifuged at 16,000 *g* for 10 min at 4°C to remove cellular debris. Protein samples (50 μg) were transferred to 96-well plates. Reactions were initiated by the addition of the assay buffer containing: 50 mM KCl, 10 mM Hepes (pH 7.5), and 0.3 mM 5,5-dithiobis nitrobenzoic acid (Invitrogen, Carlsbad, CA), in a final volume of 200 μl. Plates were immediately loaded into a temperature-controlled (37°C) SpectraMax i3x microplate reader (Molecular Devices, Sunnyvale, CA), and the absorbance at 412 nm was monitored for 20 min. Values of initial velocity (V_0) were used to determine steady-state values of K_m and V_{max} calculated according to the Michaelis-Menten equation (10).

ACSL activity

ACSL activities were measured by using liver homogenates (11). Frozen liver samples (100 mg) were homogenized in ice-cold Medium I buffer containing 10 mM Tris (pH 7.4), 250 mM sucrose, 1 mM EDTA, and 1 mM DTT. Reactions were conducted in glass vials, each with 200 μl of assay buffer containing 0.1 μCi [^{14}C]palmitate (55 μCi/μmol; American Radiolabeled Chemicals Inc., St. Louis, MO) and 50 μM palmitate in a buffer containing 0.5 mM Triton X-100, 200 mM Tris (pH 7.4), 12 mM $MgCl_2$, 1 mM EDTA, 5 mM DTT, 5 mM ATP, and 250 mM CoA. Reactions were initiated by the addition of 2–4 μg of protein followed by 10 min incubation at room temperature. One milliliter of Dole's reagent (isopropanol:heptanes:H_2SO_4, 40:10:1) was used to stop the reaction. After the addition of 2 ml of heptanes and 0.5 ml of distilled water, samples were centrifuged at 450 *g* for 5 min, and the lower inorganic phase was transferred to a new vial. Samples were then washed with 2 ml of heptanes, and 0.5 ml aliquots were combined with 4 ml of Ecoscint H scintillation solution (National Diagnostics,

Atlanta, GA) for quantification by using an LS6000IC liquid scintillation counter (Beckman Coulter; Danvers, MA).

GPAT activity

Glycerol-3-phosphate acyl transferase (GPAT) activities were measured by using isolated liver membrane fractions (12). Frozen liver samples (100 mg) were homogenized in a Potter-Elvehjem tube (10 strokes) in ice-cold Medium I buffer. Samples were centrifuged at 3000 *g* for 15 min at 4°C, and total membrane fractions were isolated from the supernatant by centrifugation at 150,000 *g* for 1 h at 4°C. GPAT activity was assayed for 10 min at room temperature in a 200 μl mixture containing 1.5 μCi [^{3}H]glycerol-3-phosphate (60 mCi/μmol; American Radiolabeled Chemicals Inc.), supplemented with: 0.8 mM glycerol-3-phosphate, 0.8 mM palmitoyl-CoA, 75 mM Tris (pH 7.5), 4 mM $MgCl_2$, 1 mg/ml fatty acid-free albumin, 1 mM DTT, and 8 mM NaF (12). Reactions were initiated by the addition of 5–10 μg of membrane protein to the assay mixture, followed by 10 min incubations at room temperature. Reaction products were extracted into chloroform and 1% perchloric acid (13), and the radioactivity present in the organic phase was determined by scintillation counting.

Rates of fatty acid oxidation

Fatty acid oxidation rates were measured in freshly collected liver samples (14). Tissues (100 mg) were homogenized in a Potter-Elvehjem tube (10 strokes) in the presence of 1 ml of ice-cold Medium I buffer without DTT, followed by centrifugation at 420 *g* for 10 min at 4°C. Supernatants (15–30 μl) were transferred to Eppendorf tubes containing 370 μl of fatty acid oxidation assay mixture containing (0.4 μCi [^{14}C]palmitate (55 μCi/μmol; American Radiolabeled Chemicals Inc.), 0.5 μM palmitate, 0.7% BSA (wt/vol), 100 mM sucrose, 10 mM Tris (pH 8.0), 5 mM KH_2PO_4, 0.2 mM EDTA, 80 mM KCl, 1 mM $MgCl_2$, 2 mM L-carnitine, 0.1 mM malate, 0.05 mM CoA, 2 mM ATP, and 1 mM DTT. Samples were incubated at 37°C for 30 min and then transferred to Eppendorf tubes containing 200 μl of 1 M perchloric acid and shaken for 1 h at room temperature. The [^{14}C]CO_2 produced by complete oxidation of radiolabeled fatty acids was trapped onto filter papers soaked with 20 μl of 1 M sodium hydroxide. Partially oxidized acid-soluble metabolites were separated by centrifugation at 14,000 *g* for 10 min at 4°C. Aliquots of the supernatants (400 μl) and paper filters were placed into separate vials containing 4 ml Ecoscint H and subjected to scintillation counting.

Hepatic TG secretion rates

Rates of hepatic TG secretion were determined in mice that were fasted for 5 h (9). The lipoprotein lipase inhibitor Tyloxapol (500 mg per kg of body weight) (Sigma-Aldrich, St. Louis, MO) was administered by tail vein injection during the light cycle. Tail tip blood samples (25 μl) were collected into Eppendorf tubes containing EDTA prior to Tyloxapol injection and at regular intervals for up to 4 h. Plasma TG concentrations were determined by using the enzymatic assays described above. Rates of hepatic TG secretion were calculated from the time-dependent linear increases in plasma TG concentration following Tyloxapol administration (15).

Glucose, insulin, and pyruvate tolerance tests

Glucose tolerance tests (GTTs), insulin tolerance tests (ITTs), and pyruvate tolerance tests (PTTs) were performed as described (16). In brief, mice were fasted with free access to water overnight (16 h) for GTTs and PTTs and 4 h during the light cycle for ITTs. Blood (<5 μl) was collected from the tail tip prior to and at regular intervals up to 120 min following intraperitoneal injection with either 1 mg/kg (high-fat-fed mice) or 2 mg/kg (chow-fed mice) glucose, 0.75 U/kg insulin, or 2 g/kg pyruvate per body mass for GTTs, ITTs, and PTTs, respectively, each dissolved in PBS. Plasma glucose concentrations were determined by using a glucometer (General Electric, Ontario, CA).

Metabolic monitoring

Mice housed in temperature-controlled cabinets with a 12 h light/dark cycle were monitored by using the Promethion Metabolic Screening System (Sable Systems International, North Las Vegas, NV). Mice were single-housed with cage floors in place of bedding and had ad libitum access to diet and water. Rates (milliliters per kilogram per hour) of O_2 consumption (VO_2) and CO_2 production (VCO_2) were determined at 5 min intervals. Respiratory exchange ratio (RER) values were calculated as VCO_2/VO_2. Mice were studied for 72 h at ambient temperatures of 30°C, 22°C, and 4°C, where the first 48 h period was considered as an acclimation period followed by a 24 h data-recording period (17). Rates of energy expenditure (kilojoules per hour) were calculated from gas exchange, and physical activities (17) were measured by the number of beam breaks per hour. Cumulative values of VO_2, VCO_2, energy expenditure were calculated and adjusted by ANCOVA (18) using VassarStats (www.vassarstats.net) to adjust for differences in lean body mass using lean body composition determined by magnetic resonance imaging (3in1 Body Composition Analyzer, EchoMRI, Houston, TX). Rates of food consumption were measured gravimetrically.

Rates of oxygen consumption by cultured hepatocytes

Oxygen consumption rates (OCR) were measured in primary hepatocytes by using an XF^{e}96 extracellular flux analyzer (Seahorse Bioscience, North Billerica, MA). Hepatocytes (7,500 cells) were seeded per well (6–8 replicates) in customized Seahorse 96-well plates. Cells were incubated in Medium 199 (Invitrogen, Carlsbad, CA) with 10% FBS and 1% penicillin-streptomycin for 4–5 h prior to commencing treatments. One hour prior to the assay, the medium was changed to XF Base Medium. BSA-conjugated palmitate was prepared (5). In selected experiments, the carnitine palmitoyltransferase 1 (CPT1) inhibitor etomoxir (200 μM) or vehicle (water) was added to wells on the microplate 15 min prior to OCR measurements. BSA as vehicle only or conjugated with palmitate (300 μM) (1:6 molar ratio) was prepared as previously described (19) and added immediately prior to initiating the assay. To test mitochondrial function, basal and maximal OCR values were assessed. To measure maximal OCR capacity, cells were first exposed to the ATP synthase inhibitor oligomycin (2 μM) to negate the portion of basal respiration used to drive ATP production. The cells were then treated with the mitochondrial uncoupler carbonyl cyanide-p-trifluoromethoxyphenylhydrazone (FCCP) (1 μM), which forces the electron transport chain to operate at maximum capacity. Once the cells achieved maximal respiratory capacity, they were treated with the electron transport inhibitors antimycin plus rotenone (1 μM), which inhibits mitochondrial respiration. Areas under the curve (AUCs) were calculated to represent respective OCRs.

Immunoblot analysis

Tissues or cells were homogenized in RIPA buffer containing 1% Nonidet P-40, 0.1% sodium deoxycholate, 0.1% SDS, 150 mM NaCl, 50 mM Tris-HCl (pH 8.0), and 2 mM EDTA with Halt Protease Inhibitor Cocktail (Thermo Fisher Scientific, Waltham, MA). Cytosolic fractions were prepared by ultracentrifugation (4). For apolipoprotein B (apoB) measurements, 2 μl of plasma was added directly to the loading buffer. Proteins were separated by SDS-PAGE and then subjected to electrophoretic transfer to nitrocellulose membranes by using standard protocols. Immunoblots

were incubated overnight with primary antibodies against Them1 (4, 6), GAPDH (Imagenex, San Diego, CA), β-actin (Sigma-Aldrich, St. Louis, MO), or apoB (BioDesign, Memphis, TN) in TBS-Tween-20 containing 3% dried milk plus 1% BSA. The blots were then probed with secondary mouse or rabbit antibodies (Dako-Agilent, Santa Clara, CA) for 1 h and detected by using enhanced chemiluminescence (SuperSignal West DURA, Thermo Fisher Scientific).

qPCR

Total RNA was isolated from samples (9), treated with RNase-free DNase I (Invitrogen), and used to synthesize cDNA (Applied Biosystems, Foster City, CA). qPCR was performed by using specific primers for the target genes and SYBR Green as the reporter dye (Applied Biosystems). Ribosomal protein L32 (RPL32) gene amplification was used for normalization. Primer sequences have been described previously (9, 11, 16, 20–22). Primer efficiencies and qPCR inhibition were determined (23). Amplification specificity analysis and qPCR controls to detect contaminations were conducted according to Minimum Information for Publication of Quantitative Real-Time PCR Experiments guidelines (24).

Statistical analyses

Data are presented as mean values with error bars representing SEM. Statistical significance was determined by using two-tailed unpaired student *t*-test when comparing two groups, with $P < 0.05$ considered to be significant, or using one-way ANOVA followed by Bonferroni multiple comparisons test when comparing three or more groups (GraphPad Prism 7; GraphPad Software, Inc., La Jolla, CA).

RESULTS

Development and validation of mouse strains

To explore the biological functions of hepatic Them1, we created a conditional transgenic mouse with a randomly integrated transgene, which allowed for tissue-specific cre-activated expression. The transgene was bred to a *Them1*$^{-/-}$ background (hereafter KO) and activated in liver by crossing with an Alb-cre-expressing mouse. This created mice that express Them1 exclusively in the liver (KO + LTg) (supplemental Fig. S1A and B). The expression of transgenic Them1 in the livers of chow-fed and high-fat-fed animals was confirmed by qPCR (supplemental Fig. S1C) and immunoblot analysis (supplemental Fig. S1D). Measurement of ACOT activity (supplemental Fig. S1E) provided evidence for the overexpression of active enzyme: Although no differences in K_m were detected among genotypes, there was a 25% increase in V_{max} values of liver homogenates from KO + LTg mice compared with the WT controls. Arguing against the possibility that these changes reflect compensation by other ACOTs, we observed only modest genotype-dependent changes in mRNA expression levels, on both diets, for some of the other *Acot* genes (supplemental Fig. S1F). There were no significant differences in body weight among the three genotypes fed chow or the high-fat diet (supplemental Fig. S2A). In addition, each exhibited similar body compositions (supplemental Fig. S2B, C), values of RER (supplemental Fig. S2D), food consumption (supplemental Fig. S2E), energy expenditure (supplemental Fig. S2F), and physical activity (supplemental Fig. S2G).

Them1 regulates fatty acid metabolism in the liver

We next explored a role for Them1 in hepatic fatty acid metabolism. There were small but significant increases in liver-to-body weight ratios of KO mice compared with WT mice (**Fig. 1A**). Although there were no histological differences observed (Fig. 1B), chow-fed KO mice tended toward increased hepatic FFA and TG contents in comparison to the WT animals, and this effect was reversed in KO + LTg mice (Fig. 1C, D). There were no related changes in hepatic concentrations of PL (Fig. 1E) or total or free cholesterol (Fig. 1F, G). When taken together with previous observations of increased fatty acid oxidation in BAT from *Them1*$^{-/-}$ mice (4, 5), these findings prompted us to examine whether Them1 regulates fatty acid oxidation within the liver. Because the metabolic utilization of fatty acids for either oxidation or complex lipid biosynthesis depends on its activation to an acyl-CoA form by ACSL isoforms, we first determined whether Them1 influenced ACSL activities. Activities were increased by 12% in KO animals, and this effect was eliminated in KO + LTg mice (**Fig. 2A**). Because there were no associated increases in the mRNA expression levels of any of the *Acsl* isoforms (Fig. 2B), this indicated that either protein levels or specific activities of ACSLs were suppressed by Them1. When compared with WT, there was a 15% reduction in rates of fatty acid oxidation in livers of KO mice, which were restored following liver-specific expression of Them1 in KO + LTg mice (Fig. 2C). Plasma concentrations of β-hydroxybutyrate, a ketone product of hepatic fatty acid oxidation, were also decreased in KO animals by 50%, but this was not restored by the reintroduction of Them1 expression in KO + LTg mice (Fig. 2D). These changes in fatty acid oxidation rates occurred in the absence of effects of Them1 expression on mRNA levels of *Pparα* or its transcriptional targets, *Cpt1a* and fatty acid binding protein-1 (*Fabp1*) (Fig. 2E).

In addition to changes in fatty acid oxidation, steady-state concentrations of hepatic FFAs and TGs may be influenced by changes in fatty acid uptake, synthesis, and secretion. Relative rates of fatty acid uptake were inferred from plasma FFA concentrations, as well as the expression of genes that mediate fatty acids uptake into hepatocytes. Suggestive of increased rates of uptake, plasma FFA concentrations were increased in the absence of Them1 expression and restored by liver-specific expression (**Fig. 3A**). However, there were no changes in mRNA levels of fatty acid transport protein (*Fatp2* or *Fatp5*) or cluster of differentiation-36 (*Cd36*) (Fig. 3B), which are the principal fatty acid transporters expressed on hepatocyte plasma membranes (25).

We next explored evidence for increases in rates of fatty acid and TG synthesis. However, there were no systematic differences observed in the mRNA expression levels of the lipogenic transcription factors, carbohydrate-responsive element-binding protein *(Chrebpα* and *Chrebpβ*) and *Srebp1c*, or in their target genes, fatty acid synthase (*Fasn*), acetyl-CoA

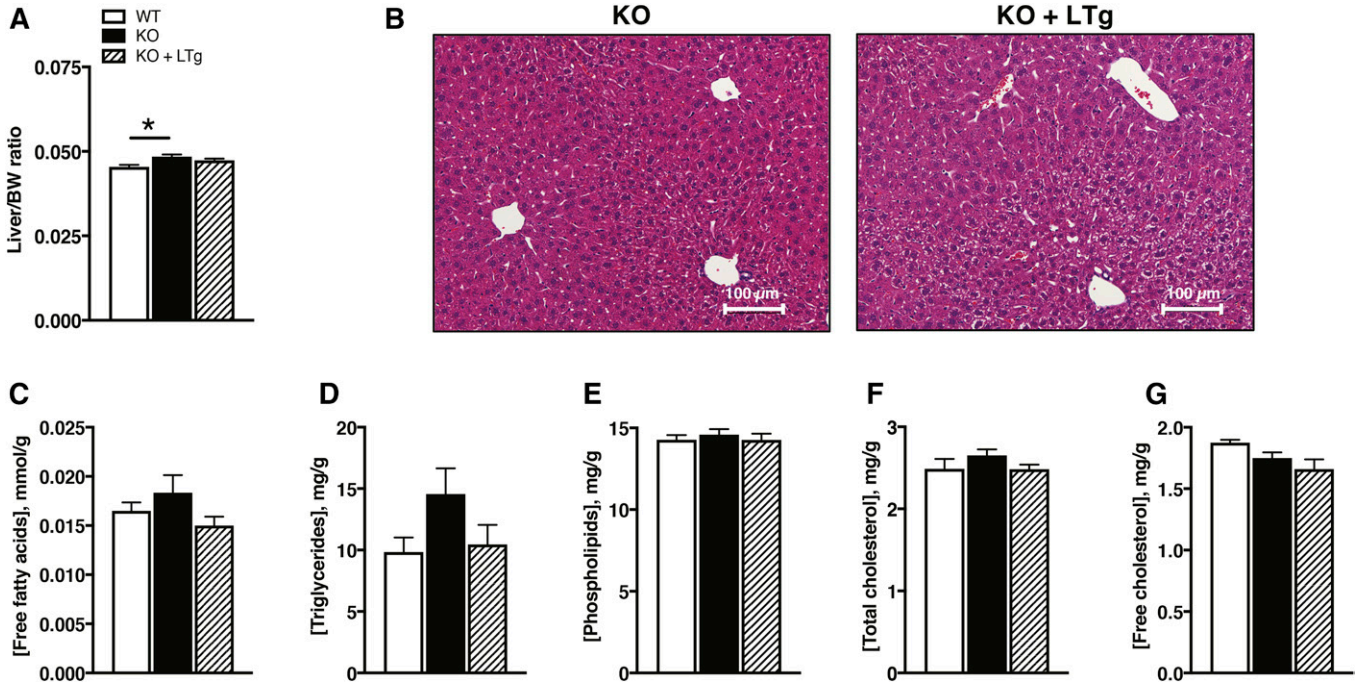

Fig. 1. Modest suppression of FFA and TG concentrations by Them1 in livers of chow-fed mice. Chow-fed mice were sacrificed at age 18 weeks. Analyses included liver-to-body weight (BW) ratios (n = 10–12 mice per group) (A) and representative light microscopic images of H&E-stained sections of livers (B), as well as hepatic concentrations (n = 6 per group) of FFAs (C), TGs (D), PLs (E), total cholesterol (F), and free cholesterol (G). * $P < 0.05$.

carboxylase (*Acc*), and stearoyl-CoA desaturase-1 (*Scd1*) (Fig. 3C). There were also no changes in the activities of GPAT (Fig. 3D), which catalyze the rate-limiting step in the synthesis of glycerolipids, including TGs and PLs (26).

Secretion of FAs into the plasma occurs in the form of TG-rich, apoB48 and apoB100-continaining VLDL particles, which also contain cholesterol. KO and KO + LTg mice exhibited nonsignificant increases in steady-state plasma TG concentrations compared with the control WT animals (Fig. 3E). KO mice also exhibited a 16% reduction in plasma cholesterol concentrations (Fig. 3F), a phenotype that was rescued in KO + LTg mice. ApoB48 expression in the plasma (Fig. 3G) correlated with the trends observed for plasma TG concentrations (Fig. 3E): Plasma apoB48 concentrations were increased in KO and KO + LTg mice by 2- and 4-fold, respectively. Although plasma apoB100 concentrations followed the same trend, there were no significant changes (Fig. 3G). Since most plasma cholesterol in chow-fed mice is carried in TG-poor HDL particles, the differing trends in plasma cholesterol compared with TGs and apoB most likely reflect the modest effect of Them1 on steady-state HDL cholesterol concentrations that we have previously reported (4). In chow-fed mice, there was a 46% increase in the rates of VLDL-TG secretion in KO mice compared with its WT controls. This was reversed when Them1 expression was restored in livers of KO + LTg mice (Fig. 3H). We did not measure apoB secretion as part of our assessment of hepatic TG secretion rates. However, because plasma apoB concentrations vary in proportion to plasma TG concentrations, it is likely that hepatic Them1 regulated both TG and apoB secretion.

Liver-specific Them1 expression promotes diet-induced hepatic steatosis

We next examined the influence of Them1 expression on the development of hepatic steatosis in response to high-fat feeding. In keeping with the increased mRNA expression (supplemental Fig. S1C), Them1 protein expression in the livers of WT mice was induced by high-fat feeding (**Fig. 4A**). In high-fat-fed mice, liver-to-body weight ratios tended to increase slightly in KO mice, but were more substantially elevated in KO + LTg mice (Fig. 4B). Histological analysis revealed an increased abundance of LDs in high-fat-fed KO + LTg mice (Fig. 4C). There were no genotype-related changes in hepatic concentrations of FFA (Fig. 4D). In contrast to previous observations in *Them1*$^{-/-}$ mice on a mixed 129/B6 genetic background (4), the absence of Them1 in KO mice did not appreciably reduce hepatic TG concentrations compared with the WT controls. However, Them1 expression in livers of KO + LTg mice increased TG concentrations in liver by 2-fold (Fig. 4E). There was a 30% reduction in hepatic PL concentrations in KO + LTg mice (Fig. 4F), whereas hepatic concentrations of total (Fig. 4G) and free cholesterol (Fig. 4H) were unchanged.

There were no appreciable changes in hepatic ACSL activities in high-fat-fed KO mice, whereas a 25% increase was observed in the KO + LTg animals (**Fig. 5A**). This occurred in the absence of changes in steady-state mRNA expression levels of *Acsl* genes (Fig. 5B). Rates of fatty acid oxidation were increased 2-fold in KO mice, and this effect was blunted in KO + LTg animals (Fig. 5C). Whereas KO mice tended to exhibit increased plasma concentrations of

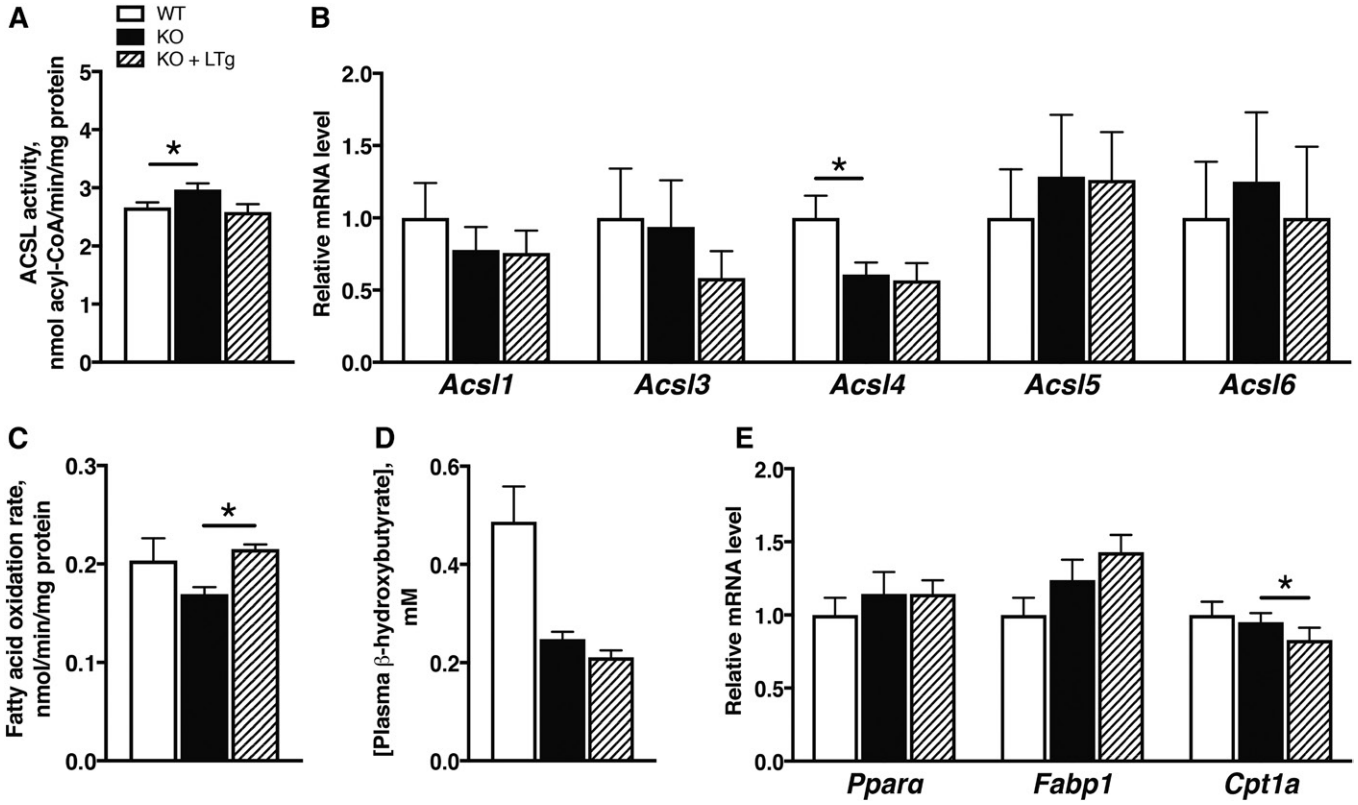

Fig. 2. Hepatic Them1 expression promotes fatty acid oxidation in livers of chow-fed mice. Chow-fed mice were sacrificed at age 18 weeks. Analyses included ACSL activity (n = 3–6 per group) (A), relative mRNA expression of *Acsl* isoforms (n = 4 per group) (B), rates of fatty-acid oxidation (n = 3–5 per group) (C), plasma concentrations of β-hydroxybutryate (n = 6 per group) (D), and relative mRNA expression of *Pparα* and its target genes (n = 4 per group) (E). * $P < 0.05$.

β-hydroxybutyrate, the reintroduction of hepatic Them1 reversed this effect (Fig. 5D). mRNA expression levels of *Pparα* tended to increase by 41% and 58% in high-fat-fed KO and KO + LTg mice, respectively, with parallel upregulation in the target genes, *Cpt1a* and *Fabp1* (Fig. 5E).

The differences observed in fatty oxidation rates led us to examine the influence of hepatic Them1 expression on mitochondrial function. Compared with WT, primary hepatocytes cultured from KO mice exhibited a 4-fold increase in basal OCR values following exposure to equal concentrations of exogenous palmitate, a response that was blunted in hepatocytes from KO + LTg mice (Fig. 5F). There was also a 2-fold increase in maximal OCR values in KO mice compared with WT that was again blunted in the KO + LTg mice (Fig. 5F). To establish that the OCR measurements primarily reflected the β-oxidation of fatty acids, hepatocytes were treated with the CPT1 inhibitor, etomoxir. For each genotype, there was no response to FCCP and no measurable differences in their basal or maximal respiration following etomoxir treatment, confirming that fatty acids were oxidized by mitochondrial β-oxidation (Fig. 2F).

Arguing against a change in fatty acid uptake, there were no systematic Them1-dependent changes in plasma FFA concentrations (Fig. 5G) or mRNA expression of fatty acid transporters in mouse livers (Fig. 5H). Similarly, there were no consistent genotype-dependent changes in lipogenic transcription factors or their target genes (Fig. 5I). The exceptions were that mRNA concentrations of *Cd36* (Fig. 5H) and *Scd1* (Fig. 5I), which are also targets of *Pparα*, increased in livers of KO and KO + LTg mice. Unlike in their chow-fed counterparts, high-fat-fed KO mice exhibited an 18% increase in GPAT activities compared with WT control and KO + LTg animals (Fig. 5J).

There were decreases in plasma TG and total cholesterol concentrations of 26% and 40%, respectively, in KO mice compared with WT controls, and this effect was reversed in KO + LTg animals (Fig. 5K, L). Similarly, the plasma concentrations of apoB48 and apoB100 were decreased in the KO mice by 12% and 27%, respectively, relative to WT animals, and were restored by the transgenic expression of Them1 (Fig. 5M). We were unable to measure hepatic rates of TG secretion in high-fat-fed mice. This may be explained by observations in rats that high-fat feeding reduces TG secretion rates apparently by channeling hepatic fatty acids away from VLDL assembly in favor of β-oxidation (27, 28).

Effects of liver-specific Them1 expression on glucose homeostasis

Finally, we examined whether Them1 expression in the liver influences glucose homeostasis. Compared with controls, fasting glucose concentrations were increased by 29% in chow-fed KO mice and tended to remain elevated in KO + LTg mice (**Fig. 6A**). There was also a trend toward decreased plasma insulin concentrations in chow-fed KO

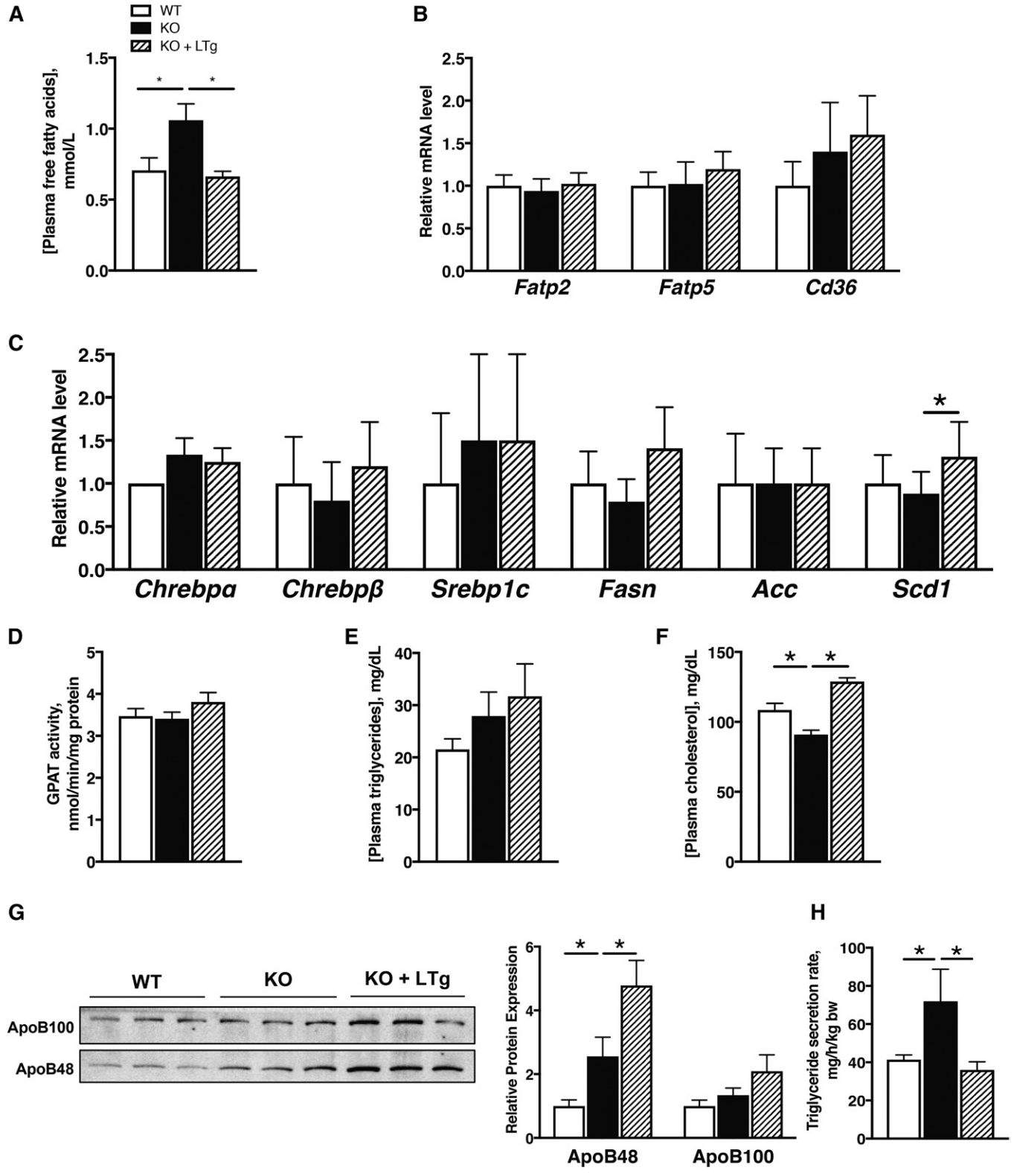

Fig. 3. Them1 expression in livers of chow-fed mice reduces hepatic TG secretion rates. Chow-fed mice were sacrificed at age 18 weeks. Analyses included plasma concentrations (n = 6 per group) of FFAs (A), mRNA expression of FATPs (B), and lipogenic transcription factors and target genes (C) (n = 4 per group). Hepatic activities of GPAT (D) (n = 4 per group), as well as plasma concentrations of TGs (E) and cholesterol (F). G: Immunoblot analysis of apoB48 and apoB100 expression in the plasma (n = 3 per group). H: Rates of plasma TG secretion measured following injecting tyloxapol in 18-week-old chow-fed mice. * $P < 0.05$. bw, body weight.

mice (Fig. 6A). By contrast, there was a modest 17% increase in fasting glucose concentrations of high-fat-fed KO + LTg mice (Fig. 6B). Plasma insulin concentrations tended to increase by 19% in KO mice and increase by 47% in high-fat-fed KO + LTg mice compared with WT mice (Fig. 6B). Although there were no changes in forkhead box protein-O1

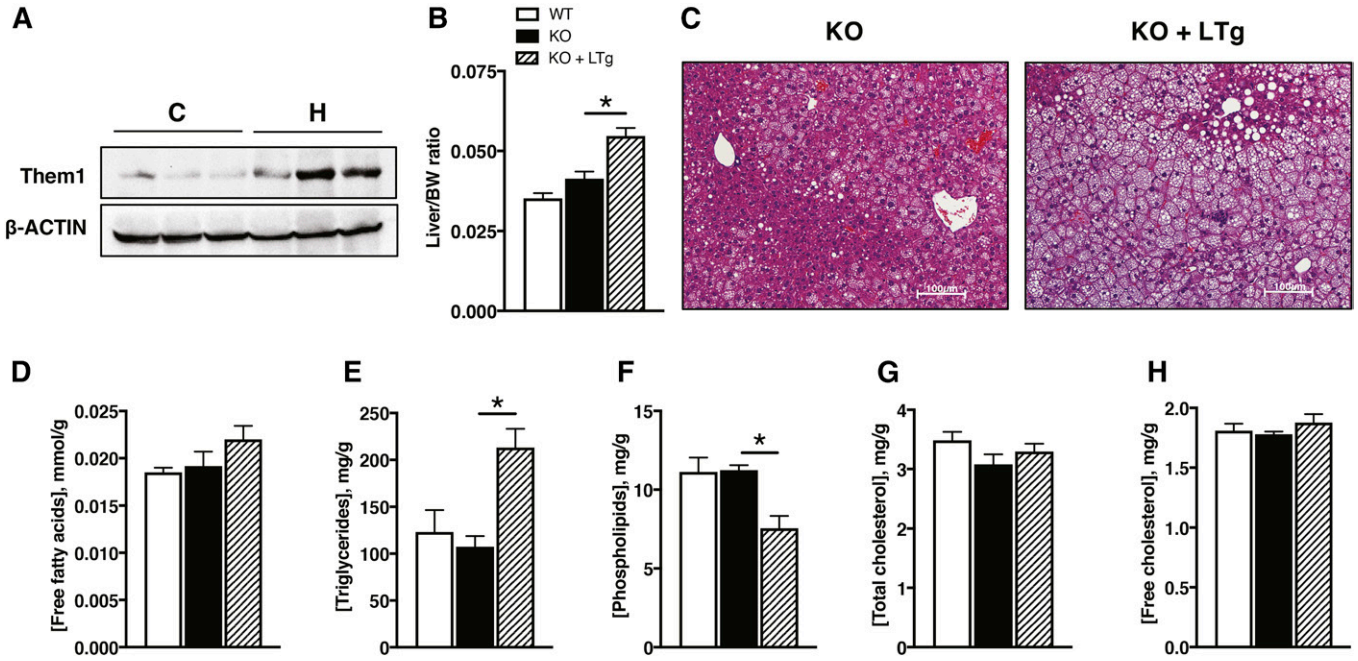

Fig. 4. Liver-specific Them1 expression promotes hepatic steatosis in high-fat-fed mice. Mice were fed a high-fat diet for 14 weeks and sacrificed at age 18 weeks. Analyses included immunoblot analysis of Them1 expression in chow and high-fat-fed WT mice (A), liver-to-body weight (BW) ratios (B) (n = 10–12 per group), and representative light microscopic images of H&E-stained sections of livers (C), as well as hepatic concentrations (n = 6 per group) of FFAs (D), TGs (E), PLs (F), total cholesterol (G), and free cholesterol (H). * $P < 0.05$.

(*Foxo1*) mRNA, there was 2.5-fold upregulation in the gluconeogenic genes phosphoenolpyruvate carboxykinase (*Pepck*) and glucose-6-phosphatase (*G6p*) in high-fat-fed KO + LTg mice (Fig. 6C). Neither glucose nor insulin tolerance differed among genotypes on either chow or high-fat diets (Fig. 6D, E). As assessed by PTTs, chow-fed KO mice tended to exhibit increased rates of hepatic glucose production, and this effect was reversed by reintroducing Them1 expression in the liver (Fig. 6F). In keeping with the high-fat-diet-induced upregulation of gluconeogenic genes, AUC values were increased for KO + LTg mice (Fig. 6F).

DISCUSSION

This study was designed to understand the specific functions of Them1 in liver and the extent to which these contribute to the phenotypes observed in *Them1*$^{-/-}$ mice (4, 5), especially the improved metabolic profiles exhibited in high-fat-fed animals (4). Our main finding was that Them1 plays a regulatory role in the hepatocellular trafficking of fatty acids (**Fig. 7**). Although it does appear to contribute to hepatic steatosis in high-fat-fed mice, Them1 overexpression in liver did not influence energy expenditure, nor did it have a significant impact on glucose homeostasis or insulin sensitivity.

The mouse model we developed for testing hepatic Them1 function proved to have both strengths and limitations. In functional experiments, where the reintroduction of Them1 into livers of KO mice reversed the phenotype of the KO mouse relative to the WT controls, the restoration of the WT phenotype provided insights into the metabolic functions of Them1. In other experiments, where unique phenotypes were observed in the setting of liver-specific overexpression, the effects were likely due to the supraphysiologic levels of Them1, although we cannot exclude possible effects on the expression of other genes that might have been affected by the insertion of the transgene. In addition, certain phenotypes of mice lacking Them1 developed for this study (KO) mice did not phenocopy *Them1*$^{-/-}$ mice originally characterized in our laboratory (4). Most notably, there was a lack of appreciable weight loss and an absence of increased energy expenditure of high-fat-fed KO mice at room temperature when compared with their respective conditional transgenic controls (WT). These differences were likely attributable to the distinct genetic backgrounds of mice in the current experiments compared with the mice we originally described. *Them1*$^{-/-}$ mice in the current study were on a pure C56BL/6J background, and WT mice were also generated in C56BL/6J mice. By contrast, in our original report (4), *Them1*$^{-/-}$ mice and their littermate controls were prepared and studied on a mixed 129/B6 genetic background, and these two genetic strains exhibit differences in susceptibility to diet-induced obesity (3, 29, 30). The changes in phenotype proved to be fortuitous because they allowed us to ascribe phenotypic differences among the three mouse genotypes to Them1 expression in the liver.

Experiments utilizing chow-fed mice provided insights into the normal metabolic role for Them1 in hepatic fatty acid metabolism. Previous studies from our laboratory have identified a role for the mitochondria-associated Them2 in generating FFAs that become substrates for ACSL1 (2, 8). Fatty acyl-CoAs are taken up into mitochondria following thioesterification by ACSL1, which interacts with the fatty

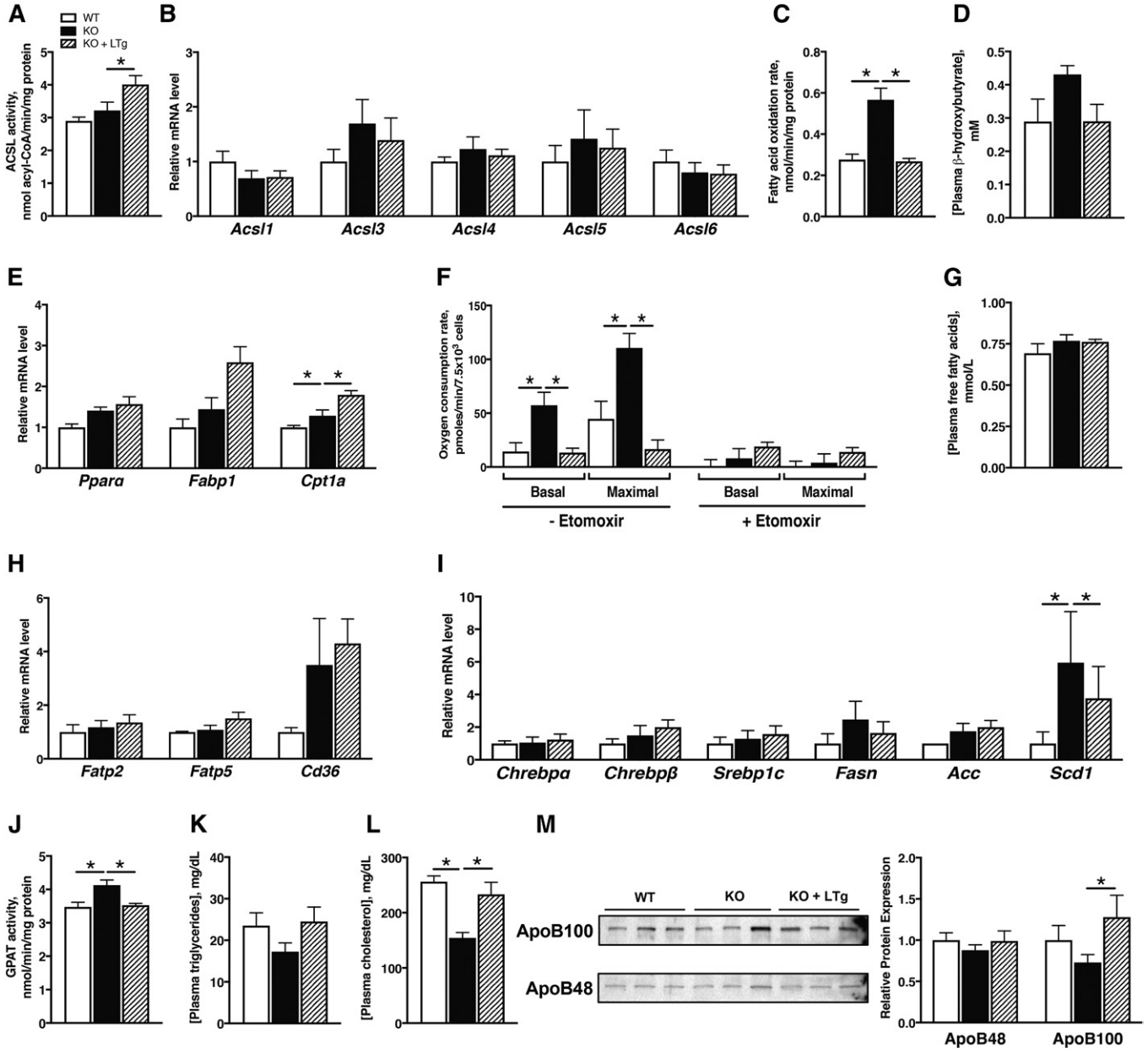

Fig. 5. Them1 expression suppresses fatty-acid oxidation in livers of high-fat-fed mice. Mice were fed a high-fat diet for 14 weeks and sacrificed at age 18 weeks. Analyses included ACSL activity (A) (n = 3–6 per group), relative mRNA expression of *Acsl* isoforms (B) (n = 4 per group), rates of fatty acid oxidation (C) (n = 3–5 per group), plasma concentrations of β-hydroxybutryate (D) (n = 6 per group), and relative mRNA expression of *Pparα* and its target genes (E) (n = 4 per group). F: Basal and maximal OCR values were measured in primary cultures hepatocytes isolated from 12-week-old mice (representative of n = 2 independent experiments, 6–8 replicates per experiment) following exposure to 300 μM palmitate, with or without being treated with the CPT1 inhibitor, etomoxir. Additional analyses using the high-fat-fed mice were plasma concentrations of FFAs (G) (n = 6 per group); mRNA expression of fatty acid transporter (H) and lipogenic transcription factors and target genes (I) (n = 6 per group); as well as GPAT activities (J) (n = 4 per group) and plasma concentrations of TGs (K) and cholesterol (L) (n = 6 per group). M: Immunoblot analysis of apoB48 and apoB100 expression in the plasma (n = 3 per group). * $P < 0.05$.

acyl-CoA transporter CPT1a in the outer mitochondrial membrane (1, 31) or, depending upon nutritional status, incorporated into glycerolipids by that activity of GPAT (1). Our current findings suggest that Them1 may function similarly. Although the precise subcellular localization of Them1 is not known with certainty, cellular fractionation studies suggest that Them1 in liver is largely cytosolic (4). This would provide an alternative route to mitochondrial Them2 for the trafficking of FFA to ACSL1. In the absence of evidence for increased fatty acid synthesis, the observed reductions in plasma FFA concentrations in mice with livers that express Them1 suggest that the enzyme promotes trafficking of extrahepatic FFA to the mitochondria for oxidation. Additionally, the reciprocal relationship of fatty acid oxidation rates and hepatic TG secretion rates suggests that, under physiological conditions, Them1 promotes the oxidation of a fatty acid pool that would otherwise be destined for incorporation into VLDL particles.

Whereas the expression levels of Them1 in the liver are relatively low (4), they are strongly upregulated by high-fat

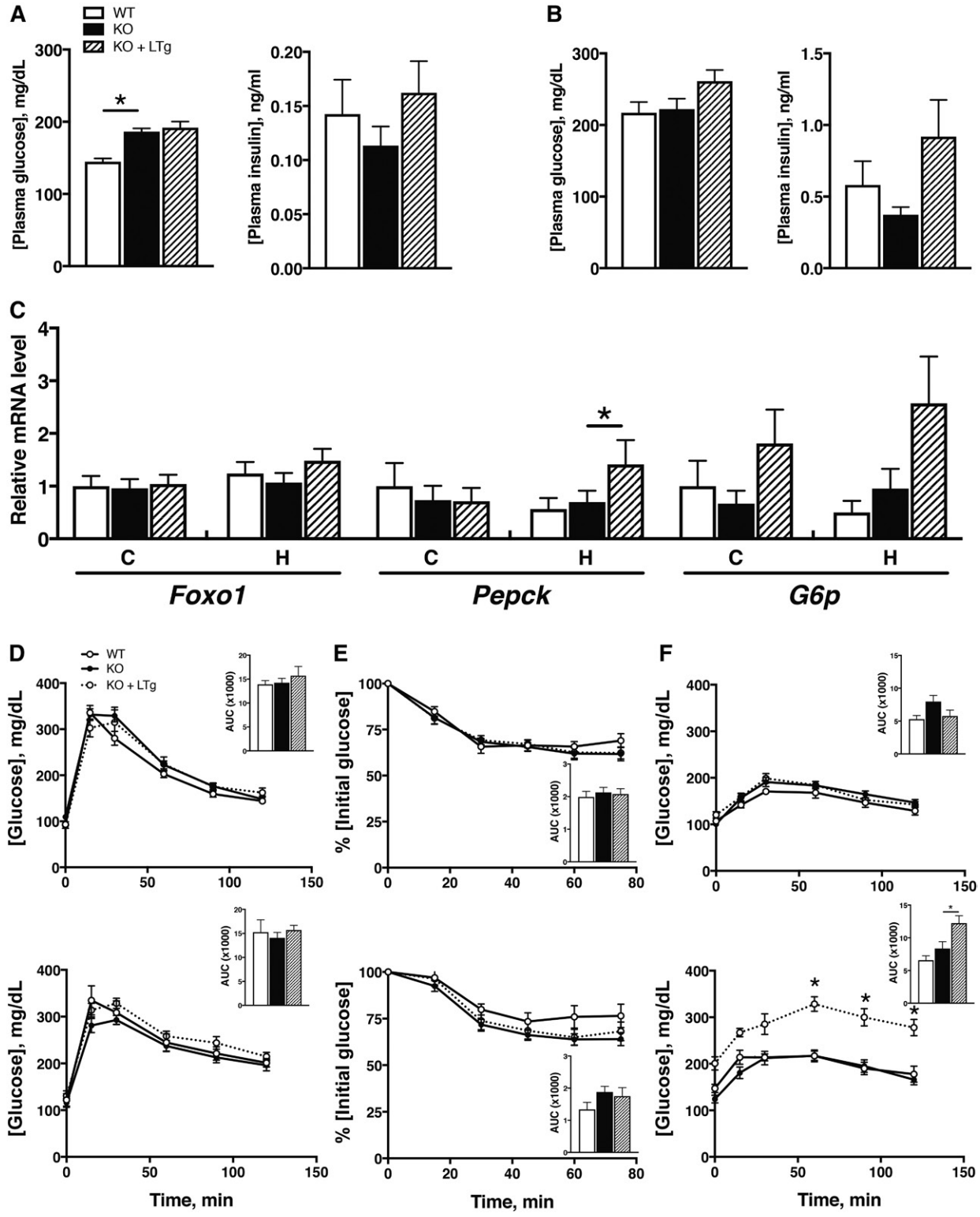

Fig. 6. Influence of hepatic Them1 expression on glucose homeostasis. Mice were fed chow or a high-fat diet for 14 weeks and studied at age 18 weeks. A, B: Fasting plasma concentrations of glucose (left) (n = 6 per group) and insulin (right) were determined in mice fed chow (A) and high-fat (B) diets. C: Relative mRNA expression of gluconeogenic genes (n = 4 per group) was determined in livers of mice fed chow (C) and high-fat (H) diets. GTTs (D), ITTs (E), and PTTs (F) were performed (n = 10–12 per group) on mice that were maintained on chow (top) or high-fat (bottom) diets. Values of AUC are shown in the inset barplots. * $P < 0.05$.

feeding (7), which also increases rates of fatty acid oxidation (32). In the current study, fatty acid oxidation rates were reduced by hepatic Them1 expression in high-fat-fed mice and in cultured hepatocytes following treatment with exogenous palmitate. Indicative of a role from Them1 in fatty acid trafficking, the increased oxidation rates in KO + LTg hepatocytes were abrogated by inhibiting CPT1. Presumably because plasma excess FFAs were circulating in

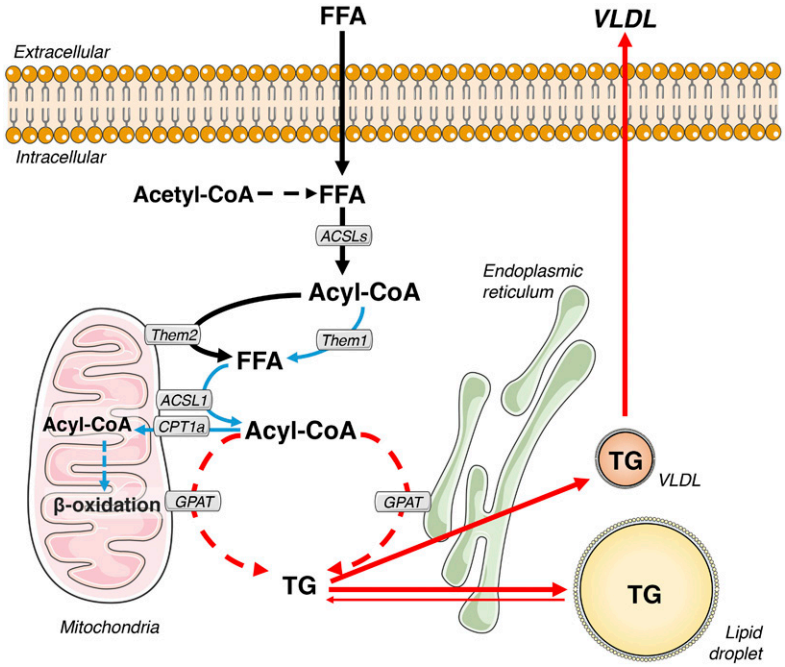

Fig. 7. Schematic model of Them1 function in hepatocellular fatty acid trafficking. Upon uptake or de novo synthesis, FFAs are activated by ACSLs in hepatocytes. Cytosolic Them1 (blue lines), as well as mitochondria-associated Them2 (black lines), selectively hydrolyze long-chain fatty acyl-CoAs to provide FFA substrates for the mitochondrial ACSL1. Under fasting conditions, ACSL1 directs acyl-CoA toward mitochondria for β-oxidation through CPT1a-dependent transport away from incorporation into VLDL TGs. By contrast, in the setting of high-fat feeding, excess fatty acyl-CoAs are directed away from mitochondria to glycerolipid synthesis by the activity GPAT (red lines), isoforms of which reside on mitochondria or endoplasmic reticulum membranes. This leads to the synthesis of TGs for incorporation into LD or VLDL particles, which are secreted into the plasma. Solid lines indicate fatty acid trafficking, and dashed lines denote biosynthetic pathways. Relative magnitudes of flux are represented by line thickness.

the setting of high-fat-diet feeding, Them1 expression did not reduce plasma concentrations. However, under these conditions, Them1 promoted the storage of fatty acids as TGs in LDs, as evidenced by an exaggerated hepatic steatosis in KO + LTg mice. Because hepatic GPAT activities were reduced by Them1 expression in high-fat-fed mice, newly synthesized TGs did not appear to be the source of excess LDs. Instead, the mechanism by which Them1 increases hepatic steatosis was more likely by suppressing lipolysis of LD TGs, such as we observed in mouse brown adipocytes in which excess FFA generated by Them1 suppressed adipose TG lipase activity following their reconversion of fatty acyl-CoAs, which functioned to suppress the activity of adipose TG lipase (5). This possibility is supported by an increase in ACSL activity in livers of high-fat-fed KO + LTg mice. Any potential increase that might have occurred in hepatic TG secretion in response to rates of reduced fatty acid oxidation was insufficient to compensate for the increased storage in LDs. In livers of high-fat-fed mice with Them1 overexpression, we also observed selective increases in mRNA expression of *Pparα* and its target genes, *Fabp1* and *Cpt1a* (33, 34). This presumably reflected the generation of excess fatty acids, which was also reflected by modest (albeit nonsignificant) increases in hepatic FFA concentrations. These changes in gene expression did not appear to have metabolic consequences because rates of fatty acid oxidation were suppressed under the same conditions.

Another issue that this study addressed was whether hepatic expression of Them1 per se was sufficient to influence glucose homeostasis, which was improved considerably in *Them1*$^{-/-}$ mice relative to littermate controls (4). We did not observe evidence that hepatic Them1 expression contributed to insulin resistance. Mice globally lacking Them1 exhibited increased insulin sensitivity when fed chow or high-fat diets, as evidenced by AUC values for both GTTs and ITTs, along with reduced values of fasting plasma glucose concentrations. Here, we observed that the expression of Them1 had no systematic effects on glucose homeostasis (4). The increases observed here in AUC values for PTTs in high-fat-fed KO + LTg mice, along with increased gluconeogenic gene expression (i.e., *Pepck* and *G6p*), likely reflects *Pparα* activation (34).

Together, the present findings establish a role for Them1 in hepatocellular trafficking of FAs, but not in the suppression of energy expenditure or regulation of glucose homeostasis. Under normal metabolic conditions, Them1 functions to direct plasma FFA toward mitochondrial β-oxidation and away from VLDL TG secretion. In the setting of high-fat feeding, Them1 promotes hepatic TG accumulation, potentially by suppressing LD lipolysis. Nonalcoholic fatty liver disease (NAFLD) is characterized by excess hepatic TG deposition and is the leading cause of liver disease worldwide (35), with current management options that remain very limited (36). Considering that upregulation of hepatic Them1 expression in the setting of overnutrition contributes to hepatic steatosis, the targeting of its enzymatic activity may be considered in the management of NAFLD.

REFERENCES

1. Grevengoed, T. J., E. L. Klett, and R. A. Coleman. 2014. Acyl-CoA metabolism and partitioning. *Annu. Rev. Nutr.* **34:** 1–30.
2. Tillander, V., S. E. H. Alexson, and D. E. Cohen. 2017. Deactivating fatty acids: acyl-CoA thioesterase-mediated control of lipid metabolism. *Trends Endocrinol. Metab.* **28:** 473–484.
3. Adams, S. H., C. Chui, S. L. Schilbach, X. X. Yu, A. D. Goddard, J. C. Grimaldi, J. Lee, P. Dowd, S. Colman, and D. A. Lewin. 2001. BFIT, a unique acyl-CoA thioesterase induced in thermogenic brown adipose tissue: cloning, organization of the human gene and assessment of a potential link to obesity. *Biochem. J.* **360:** 135–142.
4. Zhang, Y., Y. Li, M. W. Niepel, Y. Kawano, S. Han, S. Liu, A. Marsili, P. R. Larsen, C. H. Lee, and D. E. Cohen. 2012. Targeted deletion of

thioesterase superfamily member 1 promotes energy expenditure and protects against obesity and insulin resistance. *Proc. Natl. Acad. Sci. USA.* **109:** 5417–5422.
5. Okada, K., K. B. LeClair, Y. Zhang, Y. Li, C. Ozdemir, T. I. Krisko, S. J. Hagen, R. A. Betensky, A. S. Banks, and D. E. Cohen. 2016. Thioesterase superfamily member 1 suppresses cold thermogenesis by limiting the oxidation of lipid droplet-derived fatty acids in brown adipose tissue. *Mol. Metab.* **5:** 340–351.
6. Han, S., and D. E. Cohen. 2012. Functional characterization of thioesterase superfamily member 1/Acyl-CoA thioesterase 11: implications for metabolic regulation. *J. Lipid Res.* **53:** 2620–2631.
7. Ellis, J. M., C. E. Bowman, and M. J. Wolfgang. 2015. Metabolic and tissue-specific regulation of acyl-CoA metabolism. *PLoS One.* **10:** e0116587.
8. Kawano, Y., B. A. Ersoy, Y. Li, S. Nishiumi, M. Yoshida, and D. E. Cohen. 2014. Thioesterase superfamily member 2 (Them2) and phosphatidylcholine transfer protein (PC-TP) interact to promote fatty acid oxidation and control glucose utilization. *Mol. Cell. Biol.* **34:** 2396–2408.
9. Kang, H. W., M. W. Niepel, S. Han, Y. Kawano, and D. E. Cohen. 2012. Thioesterase superfamily member 2/acyl-CoA thioesterase 13 (Them2/Acot13) regulates hepatic lipid and glucose metabolism. *FASEB J.* **26:** 2209–2221.
10. Wei, J., H. W. Kang, and D. E. Cohen. 2009. Thioesterase superfamily member 2 (Them2)/acyl-CoA thioesterase 13 (Acot13): a homotetrameric hotdog fold thioesterase with selectivity for long-chain fatty acyl-CoAs. *Biochem. J.* **421:** 311–322.
11. Li, L. O., J. M. Ellis, H. A. Paich, S. Wang, N. Gong, G. Altshuller, R. J. Thresher, T. R. Koves, S. M. Watkins, D. M. Muoio, et al. 2009. Liver-specific loss of long chain acyl-CoA synthetase-1 decreases triacylglycerol synthesis and beta-oxidation and alters phospholipid fatty acid composition. *J. Biol. Chem.* **284:** 27816–27826.
12. Coleman, R. A., and E. B. Haynes. 1983. Selective changes in microsomal enzymes of triacylglycerol and phosphatidylcholine synthesis in fetal and postnatal rat liver: induction of microsomal sn-glycerol 3-P and dihydroxyacetone-P acyltransferase activities. *J. Biol. Chem.* **258:** 450–456.
13. Schlossman, D. M., and R. M. Bell. 1976. Triacylglycerol synthesis in isolated fat cells. Evidence that the *sn*-glycerol-3-phosphate and dihydroxyacetone phosphate acyltransferase activities are dual catalytic functions of a single microsomal enzyme. *J. Biol. Chem.* **251:** 5738–5744.
14. Huynh, F. K., M. F. Green, T. R. Koves, and M. D. Hirschey. 2014. Measurement of fatty acid oxidation rates in animal tissues and cell lines. *Methods Enzymol.* **542:** 391–405.
15. Vanpatten, S., G. B. Karkanias, L. Rossetti, and D. E. Cohen. 2004. Intracerebroventricular leptin regulates hepatic cholesterol metabolism. *Biochem. J.* **379:** 229–233.
16. Scapa, E. F., A. Pocai, M. K. Wu, R. Gutierrez-Juarez, L. Glenz, K. Kanno, H. Li, S. Biddinger, L. A. Jelicks, L. Rossetti, et al. 2008. Regulation of energy substrate utilization and hepatic insulin sensitivity by phosphatidylcholine transfer protein/StarD2. *FASEB J.* **22:** 2579–2590.
17. Kang, H. W., C. Ozdemir, Y. Kawano, K. B. LeClair, C. Vernochet, C. R. Kahn, S. J. Hagen, and D. E. Cohen. 2013. Thioesterase superfamily member 2/Acyl-CoA thioesterase 13 (Them2/Acot13) regulates adaptive thermogenesis in mice. *J. Biol. Chem.* **288:** 33376–33386.
18. Tschöp, M. H., J. R. Speakman, J. R. Arch, J. Auwerx, J. C. Bruning, L. Chan, R. H. Eckel, R. V. Farese, Jr., J. E. Galgani, C. Hambly, et al. 2011. A guide to analysis of mouse energy metabolism. *Nat. Methods.* **9:** 57–63.
19. Pike Winer, L. S., and M. Wu. 2014. Rapid analysis of glycolytic and oxidative substrate flux of cancer cells in a microplate. *PLoS One.* **9:** e109916.
20. Kang, H. W., K. Kanno, E. F. Scapa, and D. E. Cohen. 2010. Regulatory role for phosphatidylcholine transfer protein/StarD2 in the metabolic response to peroxisome proliferator activated receptor alpha (PPARalpha). *Biochim. Biophys. Acta.* **1801:** 496–502.
21. Zeigerer, A., R. L. Bogorad, K. Sharma, J. Gilleron, S. Seifert, S. Sales, N. Berndt, S. Bulik, G. Marsico, R. C. J. D'Souza, et al. 2015. Regulation of liver metabolism by the endosomal GTPase Rab5. *Cell Reports.* **11:** 884–892.
22. Montagner, A., A. Korecka, A. Polizzi, Y. Lippi, Y. Blum, C. Canlet, M. Tremblay-Franco, A. Gautier-Stein, R. Burcelin, Y. C. Yen, et al. 2016. Hepatic circadian clock oscillators and nuclear receptors integrate microbiome-derived signals. *Sci. Rep.* **6:** 20127.[Erratum. 2016. Sci Rep. 6: 23951.]
23. Rasmussen, R. 2001. Quantification on the LightCycler. *In* Rapid Cycle Real-Time PCR, methods and applications. S. Meuer, C. Wittwer, and K. Nakagawa, editors. Springer Press, Heidelberg. 21–34.
24. Bustin, S. A., V. Benes, J. A. Garson, J. Hellemans, J. Huggett, M. Kubista, R. Mueller, T. Nolan, M. W. Pfaffl, G. L. Shipley, et al. 2009. The MIQE guidelines: minimum information for publication of quantitative real-time PCR experiments. *Clin. Chem.* **55:** 611–622.
25. Alves-Bezerra, M., and D. E. Cohen. 2018. Triglyceride metabolism in the liver. *Compr. Physiol.* **8:** 1–22.
26. Coleman, R. A., and D. P. Lee. 2004. Enzymes of triacylglycerol synthesis and their regulation. *Prog. Lipid Res.* **43:** 134–176.
27. Francone, O. L., G. Griffaton, and A. D. Kalopissis. 1992. Effect of a high-fat diet on the incorporation of stored triacylglycerol into hepatic VLDL. *Am. J. Physiol.* **263:** E615–E623.
28. Oussadou, L., G. Griffaton, and A. D. Kalopissis. 1996. Hepatic VLDL secretion of genetically obese Zucker rats is inhibited by a high-fat diet. *Am. J. Physiol.* **271:** E952–E964.
29. Kahle, M., M. Horsch, B. Fridrich, A. Seelig, J. Schultheiss, J. Leonhardt, M. Irmler, J. Beckers, B. Rathkolb, E. Wolf, et al. 2013. Phenotypic comparison of common mouse strains developing high-fat diet-induced hepatosteatosis. *Mol. Metab.* **2:** 435–446.
30. Kless, C., N. Rink, J. Rozman, and M. Klingenspor. 2017. Proximate causes for diet-induced obesity in laboratory mice: a case study. *Eur. J. Clin. Nutr.* **71:** 306–317.
31. Lee, K., J. Kerner, and C. L. Hoppel. 2011. Mitochondrial carnitine palmitoyltransferase 1a (CPT1a) is part of an outer membrane fatty acid transfer complex. *J. Biol. Chem.* **286:** 25655–25662.
32. Kakimoto, P. A., and A. J. Kowaltowski. 2016. Effects of high fat diets on rodent liver bioenergetics and oxidative imbalance. *Redox Biol.* **8:** 216–225.
33. Mandard, S., M. Muller, and S. Kersten. 2004. Peroxisome proliferator-activated receptor alpha target genes. *Cell. Mol. Life Sci.* **61:** 393–416.
34. Kersten, S. 2014. Integrated physiology and systems biology of PPARalpha. *Mol. Metab.* **3:** 354–371.
35. Younossi, Z. M., A. B. Koenig, D. Abdelatif, Y. Fazel, L. Henry, and M. Wymer. 2016. Global epidemiology of nonalcoholic fatty liver disease—meta-analytic assessment of prevalence, incidence, and outcomes. *Hepatology.* **64:** 73–84.
36. Chalasani, N., Z. Younossi, J. E. Lavine, M. Charlton, K. Cusi, M. Rinella, S. A. Harrison, E. M. Brunt, and A. J. Sanyal. 2017. The diagnosis and management of nonalcoholic fatty liver disease: practice guidance from the American Association for the Study of Liver Diseases. *Hepatology.* Epub ahead of print. July 17, 2017; doi: 10.1002/hep.29367.